Influence of hydrogen gas over the interference of acids in inductively coupled plasma atomic emission spectrometry

Miguel Murillo *, Rosa Amaro, Alberto Fernández

Centro de Química Analítica, Escuela de Química, Facultad de Ciencias, Universidad Central de Venezuela, Apartado de Correos 47102, Caracas 1041A, Venezuela

Abstract

The effect of hydrogen gas on the plasma and its influence on acid interferences in plasma atomic emission spectrometry was studied. The study was performed with HCl and HNO_3 in the concentration range of $0-2$ mol l^{-1}. Vanadium and magnesium were used as test elements, the study was extended to other several elements. The effects of hydrogen gas on the plasma were studied by measuring excitation temperature, electron number density and the ionic-to-atomic line intensity ratio. The net effect of hydrogen was an increase in electron density and ionic to atomic line intensity ratio. A small increase in the excitation temperature was observed. The signal suppression for ionic lines causes by mineral acid was reduced when small amounts of hydrogen was introduced into the plasma as sheathing gas. This effect was attributed to the increase in plasma electron density.
© 2003 Elsevier B.V. All rights reserved.

Keywords: Atomic emission spectrometry; Inductively coupled plasma; Mineral acid interferences; Hydrogen gas plasma

1. Introduction

Mineral acid such as hydrochloric, nitric, sulfuric and perchloric are used in numerous sample decomposition procedures in ICP-AES. However, the use of a mineral acid generally leads to various types of interferences [1–25]. In general, an increase in mineral acid concentration causes a significant decrease in the emission signal observed in ICP-AES. This interference has been attributed to: a decrease in the sample aspiration rate as a result of increased viscosity [1–8], a change in nebulizer efficiency due to droplet size distribution [6,9–14,25], a variation in aerosol transport efficiency [1,4,6,8–17] and a change in plasma excitation conditions [11,18–24].

Fernandez et al. [20] reported that the magnitude of acid interferences is strongly dependent on the energy of the emission line: atomic or ionic, reporting larger effects on ionic lines. They observed that the interference depended on plasma operation conditions. In some cases, it was found that the excitation temperature remained unchanged by a function of acid concentration, while the electronic density decreased. The significant signal depression effect (up to 30% for 2 mol l^{-1}

---

* Corresponding author. Fax: +58-2-12-6934977.
E-mail address: mmurillo@strix.ciens.ucv.ve (M. Murillo).

nitric acid concentration) observed for ionic lines was attributed to changes in plasma excitation conditions.

On the other hand, the addition of hydrogen via nebulizer gas has been studied [26–28] observing an increase in the excitation temperature and electron density mainly due to the high thermal conductivity of hydrogen compared with argon.

In the present work, the effect of hydrogen on acid interferences on emission signals was studied. HNO_3 and HCl were in the concentration range of 0–2 mol l^{-1}. Four sets of operating conditions were selected by adjusting the carrier gas flow rate, the sheathing gas flow rate, power and hydrogen flow rate (see Table 1 for operation conditions). The corresponding plasma excitation conditions were assessed by measuring excitation temperature, electron number density and ionic-to-atomic line intensity ratio.

2. Experimental

2.1. Instrumental

A Jobin-Yvon JY-24 ICP emission spectrometer operating at 40 MHz and 1.3 kW. A demountable torch with a 2.5 mm i.d. alumina injector. Mass flow controllers (Brooks 5850E) replaced the original gas flow meter for the aerosol carrier and sheathing gas. Solutions were aspirated using a Meinhard nebulizer (TR-20C2) with a Scott-type spray chamber working at room temperature. A peristaltic pump was used in order to maintain sample flow rate. The amount of aspirated solution due to changes in viscosity were minimized.

Hydrogen was introduced as a sheathing gas at the exit of the spray chamber. The sheathing tube was originally designed to avoid salt deposition on the inner walls of the torch injector tube [29]. It has also been used to study energy transfer efficiency to the injected species [26,30]. Argon and hydrogen could be added to the aerosol carrier gas at the exit of the spray chamber by sheathing device. In this way, the total flow of the sheathing gas was held constant and in our experiments it was 0.30 l min^{-1}.

2.2. Temperature measurements

The Boltzmann plot method was used to measure excitation temperature. Eleven vanadium ionic lines were selected. Their wavelength, energy level and oscillator strength values were taken from references [31–33].

2.3. Electron number density

The electron number density was determined from Stark broadening of the 486.12 nm (Hβ-line) using Griem's approximation [33].

2.4. Ionic-to-atomic line intensity ratio

The Mg II 280.270/Mg I 285.213 nm intensity ratio was measured to verify plasma conditions [20].

2.5. Chemicals, emission lines and experimental procedures

Vanadium was selected, as the test element because stable aqueous solutions of vanadium

Table 1
Operating instrumental conditions and plasma excitation conditions

Condition	Aerosol carrier gas flow rate (l min^{-1})	Sheathing gas flow rate (l min^{-1})	Electronic density $\times 10^{13}$ (cm^{-3})	Excitation temperature (°K)	Mg II/ Mg I
1	0.75Ar	0.00Ar	131 $\pm$ 3	5440 $\pm$ 200	7.8 $\pm$ 0.2
2	1.00Ar	0.30Ar	48 $\pm$ 1	4560 $\pm$ 80	3.1 $\pm$ 0.2
3	1.00Ar	0.25Ar+0.05H$_2$	68 $\pm$ 1	4840 $\pm$ 70	5.2 $\pm$ 0.2
4	1.00Ar	0.23Ar+0.07H$_2$	73 $\pm$ 1	4880 $\pm$ 80	6.1 $\pm$ 0.2

could be obtained without the addition of acid, and atomic and ionic lines are well characterized. Wavelength and the excitation and ionization potentials are listed in Table 2.

Vanadium solutions were prepared at a concentration of 50 mg ml^{-1} by dilution from a concentrate prepared from NH_4VO_2 (Merck, *pro analysis* grade). Hydrochloric (37% v/v) and nitric acids (65% v/v) from Riedel-de Haën were used. Acid concentrations varied from 0 to 2 mol l^{-1}. At least three replicates with an integration time of 0.3 s were used for each solution. An equilibrium time of approximately 5–10 min was used between measurements at different acids concentrations. Net intensities were was obtained by subtracting background from gross intensity. Relative intensities (I_r) were obtained normalizing all intensities to the intensities of an aqueous solution.

3. Results and discussion

The influence of hydrogen addition on the acid effect was studied using four different sets of plasma operating conditions. Operating conditions are listed in Table 1, along with excitation temperatures, electron number densities and Mg II/Mg I intensity ratios, measured without acid concentration.

Condition 1 produces a high Mg II/Mg I ratio (robust conditions), whereas condition 2 produces a low ratio (non-robust conditions). According to those reported by Fernandez et al. [20], the influence of HCl and HNO_3 on the emission line will be different for each set of conditions. Only minor intensity depression is expected for condition 1. In contrast, significant effects is expected for condition 2. Different amounts of hydrogen were added to the sheathing gas (0.05 and 0.07 l min^{-1}) which was constant (total flow rate at 0.30 l min^{-1}). Table 1 lists these conditions as condition 3 and 4, respectively. It is important to note that even a small amount of hydrogen in the sheathing gas (0.05 l min^{-1}) resulted in approximately 30% increase in the electron density, 6% in excitation temperature and 48% in the Mg II/Mg I ratio compared with those obtained when pure argon was used in the sheathing gas (condition 2). When the hydrogen flow rate increased to 0.07 l min^{-1}, the electron density and the Mg II/Mg I ratio increased 52 and 71%, respectively. However, the excitation temperature was similar to that when 0.05 l min^{-1} of hydrogen was used.

It is clear that the use of hydrogen results in a significant increase in the electron density but not

Table 2
Wavelength, excitation and ionization potential and energy sum of different elements studied

Spectral species	Wavelength (nm)	Excitation potential (eV)	Ionization potential (eV)	Energy sum (eV)
V I	437.924	3.13	–	3.13
Mg I	285.213	4.34	–	4.34
Mn I	279.420	4.44	–	4.44
Mn I	380.672	5.37	–	5.37
Mn I	382.351	5.38	–	5.38
Cu I	221.458	6.98	–	6.98
Cu I	222.778	7.20	–	7.20
V II	309.311	4.40	6.74	10.14
V II	292.402	4.63	6.74	11.37
Mg II	280.270	4.42	7.64	12.06
Mn II	259.373	4.77	7.43	12.20
Mn II	344.198	5.37	7.43	12.80
Mn II	261.020	8.16	7.43	15.59
Cu II	224.700	8.23	7.73	15.96
Mn II	263.984	8.75	7.43	16.18
Cu II	204.379	8.78	7.73	16.51

the excitation temperature. This fact can be used to compensate the electron density decrease observed when acid solutions are introduced into the plasma [20].

The effect of HCl concentration on atomic and ionic vanadium lines was studied for condition 1, 2 and 3. As was reported earlier [20], for condition 1, the decrease in the signal was approximately 8% for both, atomic and ionic lines when increasing HCl concentration. On the other hand, for condition 2, a strong decrease (up to 40%) in ionic lines was observed in contrast to atomic lines. When hydrogen was added to the sheathing gas (condition 3), the suppression effect for ionic lines intensities were approximately 20%.

The effect of HNO_3 on vanadium line intensities was similar to that obtained for HCl and hydrogen caused the same effect, i.e. reduction of the acid depression effect.

The effect of acid interferences on several element lines having different energies sum (excitation + ionization energy) was performed using vanadium, manganese, copper and magnesium spectral lines. This study was carried out using 2 mol l^{-1} HCl and plasma conditions 2 and 3. Spectral lines and their energies are listed in Table 2. Results are normalized to those obtained without acid and plotted as a function of sum energy.
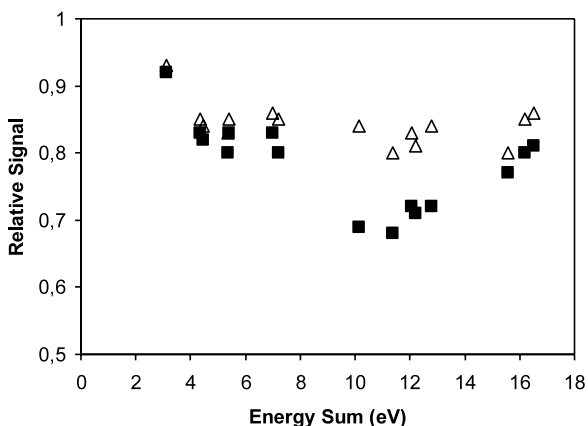

Fig. 1. Relative emission for different elements as a function of the energy sum (Eexc+Eion) under two different instrumental operating conditions. (■) Condition 2 and (△) Condition 3. 2 mol l^{-1} HCl concentration. See Table 1 for operation conditions.

Fig. 1 shows the acid effects as a function of the energy sum. For atomic lines (< 7.5 eV), the acid effect remained constant for two plasma conditions. In other words, the addition of hydrogen did not change the acid effect on the reduction emission intensities of these line. On the other hand, for the ionic line (> 7.5 eV), a significant reduction in acid effect was obtained when small amounts of hydrogen were introduced into the sheathing gas (condition 3). This effect is more noticeable for lines with excitation energies around 12 eV. Similar observations were made when hydrogen was added to the aerosol stream [26] for ionic lines with excitation energies ranged from 9 to 13 eV.

These results indicate that small amount of hydrogen in the sheath gas partly compensates the acid depressing effect, especially for ionic lines. Partly, attributed to the electron density increase. As observed in Table 1, the electron density is increased by 30% when 0.05 l min^{-1} of hydrogen is introduced as a sheathing gas but this increase is not high enough for total acid interference elimination.

Fig. 2 shows the relative signal as a function of the acid concentration (HCl) for ionic (280.270 nm) and atomic (285.213 nm) Mg lines measured under four plasma operations conditions (see Table 1 for operation conditions). The Mg ionic line was selected due to its energy sum of 12.06 eV which has the maximum interference effect (Fig. 1). Fig. 2 (a) shows that for Mg I the acid effect remains unchanged for the all plasma conditions, implying that the depressive effect on atomic line is not affected by changes in plasma operating conditions. On the other hand, Mg II (Fig. 2 (b)) exhibits a dramatic depressive effect strongly dependent on plasma operating conditions. Theses results confirm previous observations [20,34] where acid interference effects were attributed to a change in plasma conditions produced by the presence of acid in the plasma.

When hydrogen was added to the sheathing gas, a signal increase was observed (conditions 3 and 4). For the higher hydrogen flow rate (condition 4), the acid effect on the plasma excitation conditions was reduced and the emission signal was similar to that observed when robust plasma
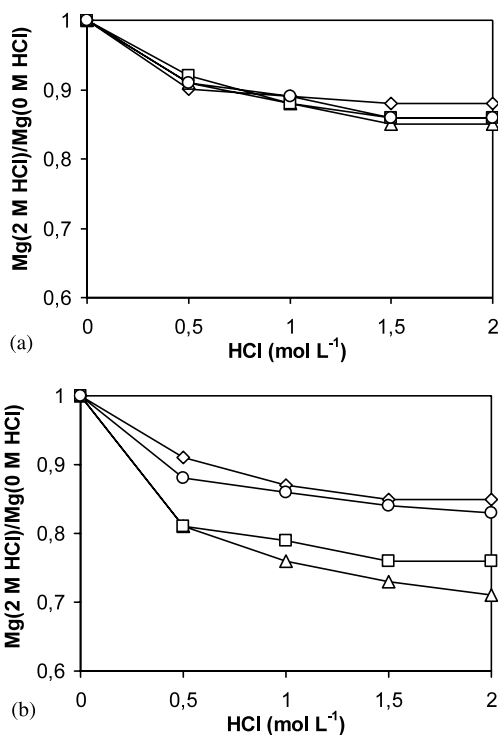
(a)

(b)

Fig. 2. Relative emission signal for Mg atomic (a) and ionic line (b) for four instrumental operating conditions ($\Diamond$) Condition 1; ($\triangle$) Condition 2; ($\square$) Condition 3; ($\bigcirc$) Condition 4. See Table 1 for operation conditions.

conditions were used. The effect of $0.07 \, \mathrm{l \, min^{-1}}$ of hydrogen in the sheathing gas resulted in a significant increase in the electron density and the Mg II/Mg I ratio.
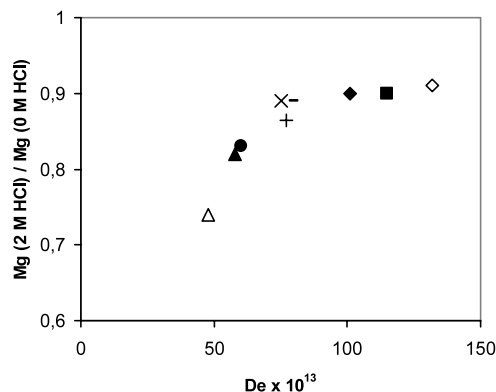

Fig. 3. Relative emission intensity for Mg II 280.270 nm line as a function of the electronic density. 2 mol $\mathrm{l^{-1}}$ HCl concentration. ($\Diamond$) Condition 1; ($\triangle$) Condition 2; ($\blacklozenge$) Condition 3; ($+$) Condition 4; ($\blacksquare$) Condition 5; ($-$) Condition 6; ($\bullet$) Condition 7; ($\times$) Condition 8 and ($\blacktriangle$) Condition 9. See Table 3 for operation conditions.

The dependence of the acid interference with electronic number density seems to be evident, yet we do not know where the acid effects are critical. In this sense, the intensity of Mg ionic line (280.27 nm, 12.04 eV) was measured at different plasma conditions that reach different electronic densities in solutions with and without acid HCl (2 mol $\mathrm{l^{-1}}$). These plasma conditions used throughout this experiment are shown in Table 3. Fig. 3 shows the intensity of Mg II (280.27 nm) relative to the intensity without acid as a function of the electron number density. Below 75×10^{13} cm^{-3}, the acid effect was drastically increased. Above this value, the acid effect was below 10%.

Table 3
Operational instrumental conditions plasma and electronic density for the experimental data as shown in Fig. 3

Plasma instrumental operational condition	Argon as aerosol carrier gas flow rate (l min^{-1})	Argon as sheathing gas flow rate (l min^{-1})	Electronic density $\times 10^{13}$ (cm^{-3})
1	0.75	0.00	132
2	1.00	0.30	48
3	0.75	0.15	101
4	0.75	0.30	77
5	0.85	0.0	115
6	0.85	0.15	80
7	0.85	0.30	60
8	1.00	0.0	75
9	1.00	0.15	58

In the present work, the electron number density did not increase with the addition of hydrogen (condition 4, Table 1) reaching a limit value observed in Fig. 3, for this reason the depressive effect caused by the acid was attributed to the decreases in electronic density. Likewise, it is important to note that the addition of hydrogen was effected by maintaining constant analyte residence times at discharge (a total sheathing gas flow of 0.30 l min^{-1}) and without altering the aerosol formation process in the nebulization stage, according to the diagnostic parameters determined, electronic density was the one mostly affected while the temperature in this experience group remained unchanged, therefore, it would be difficult to attribute it to a thermal process.

4. Conclusions

The effect produced by the acid accentuates with decreases in electronic density, especially when descending below 75×10^{13} cm^{-3}. The results indicate that small amount of hydrogen in the sheath gas partly compensates the acid depressing effect, especially for lines with an energy sum of around 12 eV.

Acknowledgements

References

[1] S. Greenfield, M. McGeachin, P.B. Smith, Anal. Chim. Acta 84 (1976) 67.
[2] R.L. Dahlquist, J.W. Knoll, Appl. Spectrosc. 32 (1978) 1.
[3] F.J.M.J. Maessen, J. Balker, J.L.M. De Boer, Spectrochim. Acta 37B (1982) 517.
[4] X.-E. Shen, Q.-L. Chen, Spectrochim. Acta 38B (1983) 115.
[5] J.L. Imbert, J.M. Mermet, Analusis 12 (1984) 209.
[6] J. Farino, J.R. Miller, D.D. Smith, R.F. Browner, Anal. Chem. 59 (1987) 2303.
[7] T.D. Hettipathirana, A.P. Wade, M.W. Blades, Spectrochim. Acta 45B (1990) 277.
[8] A. Canals, V. Hernandis, J.L. Todoli, R.F. Browner, Spectrochim. Acta 50B (1995) 305.
[9] H. Ishii, K. Satoh, Talanta 30 (1983) 11.
[10] M.A. Wandt, M.A. Pougnet, A.L. Rodgers, Analyst 109 (1984) 1071.
[11] M. Carré, K. Lebas, M. Marichy, M. Mermet, E. Pousel, J.M. Mermet, Spectrochim. Acta 50B (1995) 271.
[12] J.L. Todolí, J.M. Mermet, A. Canals, V. Hernandis, J. Anal. At. Spectrom. 13 (1998) 55.
[13] I.I. Stewart, J.W. Olesik, J. Anal. At. Spectrom. 13 (1998) 1249.
[14] S. Maestre, J. Mora, J.L. Todolí, A. Canals, J. Anal. At. Spectrom. 14 (1999) 61.
[15] G.F. Larson, V.A. Fassel, R.H. Scott, R.N. Kniseley, Anal. Chem. 47 (1975) 238.
[16] Z. Zadgorska, H. Nickel, M. Mazurkiewicz, G. Wolff, Fresenius Z. Anal. Chem. 314 (1983) 356.
[17] B. Budic, V. Hudnik, J. Anal. At. Spectrom. 9 (1994) 53.
[18] E. Yoshimura, H. Suzuki, S. Yamazaki, S. Toda, Analyst 115 (1990) 167.
[19] E.G. Chudinov, I.I. Ostroukhova, G.V. Varvanina, Fresenius Z. Anal. Chem. 335 (1989) 25.
[20] A. Fernández, M. Murrillo, N. Carrión, J.M. Mermet, J. Anal. At. Spectrom. 9 (1994) 217.
[21] I.B. Brenner, J.M. Mermet, I. Segal, G.L. Long, Spectrochim. Acta 50B (1995) 323.
[22] I.B. Brenner, I. Segal, J.M. Mermet, M. Mermet, Spectrochim. Acta 50B (1995) 333.
[23] C. Dubuisson, E. Pousseland, J.M. Mermet, J. Anal. At. Spectrom. 12 (1997) 281.
[24] C. Dubuisson, E. Pousseland, J.M. Mermet, J.L. Todolí, J. Anal. At. Spectrom. 13 (1998) 63.
[25] J.L. Todolí, J.M. Mermet, J. Anal. At. Spectrom 15 (2000) 863.
[26] M. Murillo, J.M. Mermet, Spectrochim. Acta 44B (1989) 359.
[27] A. Batal, J. Jarosz, J.M. Mermet, Spectrochim. Acta 37B (1982) 511.
[28] P.E. Walter, C.A. Barnardt, Spectrochim. Acta 43B (1988) 325.
[29] J.M. Mermet, P. Ripoche, C. Trassy, in: R.M. Barnes (Ed.), Development in Atomic Spectrochemical Analysis, Heyden, London, 1981, pp. 718–742.
[30] M. Murillo, J.M. Mermet, Spectrochim. Acta 42B (1987) 1151.
[31] C. Corliss, W. Bozmann, Experimental Transition Probabilties for Spectral Lines of Seventy Elements, NBS Monograph 53, Washinton, DC, 1962.
[32] J. Jarosz, J.M. Mermet, J. Robin, Spectrochim. Acta 33B (1978) 55.
[33] J.M. Mermet, in: P.W.J.M. Boumans (Ed.), Inductively Coupled Plasma Emission Spectroscopy, part 2, Wiley, New York, 1987, pp. 353–386.
[34] J.L. Todolí, J.M. Mermet, Spectrochim. Acta 54B (1999) 895.